RSC Advances

This is an *Accepted Manuscript*, which has been through the Royal Society of Chemistry peer review process and has been accepted for publication.

Accepted Manuscripts are published online shortly after acceptance, before technical editing, formatting and proof reading. Using this free service, authors can make their results available to the community, in citable form, before we publish the edited article. This *Accepted Manuscript* will be replaced by the edited, formatted and paginated article as soon as this is available.

You can find more information about *Accepted Manuscripts* in the Information for Authors.

Please note that technical editing may introduce minor changes to the text and/or graphics, which may alter content. The journal's standard Terms & Conditions and the Ethical guidelines still apply. In no event shall the Royal Society of Chemistry be held responsible for any errors or omissions in this *Accepted Manuscript* or any consequences arising from the use of any information it contains.

ROYAL SOCIETY OF CHEMISTRY

www.rsc.org/advances

Journal Name ARTICLE

Cite this: DOI: 10.1039/x0xx00000x

Received 00th January 2012,
Accepted 00th January 2012

DOI: 10.1039/x0xx00000x

www.rsc.org/

Molar ratios of therapeutic water-soluble phenothiazine•water-insoluble phospholipid adducts reveals a Fibonacci correlation and a putative link to structure-activity relationships

Hendrik Keyzer[a*†], Stephen John Fey[b*], Barry Thornton[c] and Jette E. Kristiansen[d#]

That non-antibiotics can sensitise microorganisms to antibiotic treatment suggests that these molecules have valuable potential to treat multiple drug resistance. Here we explore the spatial interaction of selected therapeutic phenothiazine hydrochloride derivatives (PTH) with various lipids. Micro-gravimetric titrations were used on aqueous suspensions of: promethazine (PMTZ), promazine (PMZ), triflupromazine (TFM), chlorpromazine (CPZ), prochlorperazine·HCl (PClP•HCl), thrifluoperazine·HCl (TFP•HCl), prochlorperazine·2HC1 (PClP•2HCl), trifluoperazine·2HCl (TFP•2HCl) and synthetic 1,2 diacyl-sn-glycero-3-phospholipids (PL) with even-numbered symmetric saturated diacyl chains with the headgroups: choline (PC), glycerol (PG), serine (PS), ethanolamine (PE), phosphatidic acid (PA). We observed water soluble products with replicable molar ratios (MR) that could be divided into two series. 'Series 1' (PMTZ < PMZ < CPZ < PClP < TFP) followed the ionization potential and concomitant sedative effects. 'Series 2' followed the lipophilicity of PL and could be related to non-neuronal physiological aspects. The MR of Series 2 followed the PL order PC < PG < PS < PE < PA, echoing the changes in membrane proportions found in a eukaryotic cell proceeding from the plasma membrane to the endoplasmic reticulum. The same order was found in hydrogen ion concentration increase [ΔH_i^+] when plotted against the MR for each separate diacyl series. The [ΔH_i^+] of the PTH/PL is always larger than that of the self-associated pure PTH. In summary, the reproducibility and similarity of the measurements using different PTH derivatives and PL suggests that similar adducts are formed in all cases. We propose that the PTH•PL adduct has a "helical shape" showing Fibonacci properties for molecules. These observations may open new opportunities for novel therapy developments.

RSC Advances Accepted Manuscript

Journal Name

RSCPublishing

ARTICLE

Introduction

Chlorpromazine hydrochloride (CPZ) and related exobiotic, amphipathic, micelle-forming phenothiazine (PTH) salts (see Figure 1A for representatives) have shown therapeutic effectiveness against deleterious micro-organisms and cancer cells[1,2,3,4,5 and 6]. Evidence is mounting that alone or as helper compounds, they may revive the use of the older, classical antibiotics to combat the alarming rise of multi-resistant microbes world-wide[1,5,7 and 8]. PTH, as neuroleptics, involve stereospecific sites, but their mode of action includes so-called "non-neuronal" interactions that may cover many side-effects and contribute to other psychotropic and/or biological activity[9,10,11 and 12]. Human toxicity, often a concern with PTHs, could be measured *in vitro* using 3D cultures which accurately reflect the *in vivo* response[13]. A truism exists that the longer a drug is in use the more side-effects are discovered. After all, micro-organisms have none of the above-mentioned receptors yet become "sedated" or otherwise react to PTH medicinal intervention[14,15 and 16]. Goosey and Doggett point out that PTH neuroleptics involve lipophilicity rather than solely shape-specific mechanisms[17]. The notion that the PTH accumulate in membranes heterogeneously is well-established[18 and 19]. Such amphipaths distribute into rich and poor domains in phospholipid (PL) multilayers[20,21 and 22]. For example, similar activity has been noted for alamethacin which forms micelles in aqueous solutions, and readily incorporates into plasma bilayers forming channels by self-association[23]. The critical micelle concentration of CPZ in water is about 10^{-5} M [20]. With a preference for lipids, cell lysis begins to occur at 3 x 10^{-5} M [22]. Membrane saturation may be as high as 1 M [20 and 22]. Maher and Singer showed that small amphipaths, including CPZ, at concentrations lower than those inducing lysis, promoted gross distribution of components in the plane of quite different membranes, and that this resulted in their highly selective extraction[22]. CPZ tends to accumulate in humans mainly in lecithin-rich sites, persisting unchanged up to 1 year[20,22 and 24]. PL are well-known to move in a cellular membrane[25 and 26] but accumulation of PTH at a target PL site, as one would expect from a PTH-enriched domain, may well immobilize the PL (sedate), extract it (inducing lysis), penetrate into, or otherwise disrupt its behaviour in the membrane. Carey and coworkers showed that CPZ•HCl solubilized membrane PL efficiently as micellar solutions when the drug/PL molar ratio reached 4:1 [27]. We found a similar effect with phosphatidylcholine (PC), phosphatidyl glycerol (PG) and an exobiotic, synthetic lipid, discovering in the process, that the molar solubilization of PL by PTH was quite reproducible[28]. Therefore, we deemed that a study is warranted, focusing on the effect of various quantities of aqueous PTH *in vitro* on some major PL groups found in most eukaryotic and prokaryotic membranes. We also wish to examine some putative structure activity relationships (SAR) other than neurolepticity and propose higher order structures for the PTH–PL interactions.

Results

The molar ratios (MR) in Table 1 are generally averages of triplicates. All PTH/PL interaction product MRs were replicable to within ±5%. The use of hydrochloride salts was justified: for example, PCLP as the hydrochloride has a PTH/PL MR comparable to that of the edysilate derivative but the maleate derivative yielded an immediate dense precipitate resisting all further addition of PTH to reach an MR. The adducts were generally stable, *i.e.* did not precipitate until the MR increased for the most part beyond about 40-50 at which point the initially soluble adducts tended to precipitate after 2 to 24 hours, (precipitation is indicated by the underscored values in Table 1) probably due to splaying of the longer chains. Above the PL 18C, MR endpoint errors generally tended to increase.

Figure 2 is a plot with error bars of CPZ/PL MR *vs* PL molecular weight (MW). The replicability of the MR data suggested that the PTH/PL products may well be designated as adducts rather than by the looser term aggregates, especially in view of the notion that we may not just be dealing with micelles *per se.* Advisedly, and henceforth, we eschew the term "micelle" wherever possible[29]. More evident from Table 1 than from Figure 2 is that the CPZ/PL adduct MR for comparative Ci (carbon atoms per chain) always increases in the headgroup order PC < PG < PS < PE< PA. All PTH/PL adducts exhibited similar profiles. Thus, we believe that similar conformational structures are involved. Table 1 shows the MR of various PTH sequestering PL (C16), and extracts. For the pure PL involved, on the whole, all the PTH/PL MR followed the same trend: PMTZ > PMZ > CPZ > TFM > PClP >TFP, including PI, and *E. coli* B. Since characteristic charge transfer complex adduct colours were observed especially for the extracts, developing slowly and deepening on cooling to 0 °C, we concluded that the PTH in their adducts followed excimeric charge transfer complex regimes, as they do in the pure form[20]. However, charge transfer is confined to the PTH molecules. We found that this phenomenon extended to all the analogues of CPZ in our study, and suggested a universal trait[30].

Solid state aspects

Tehrani and coworkers claimed to have observed CPZ nanocrystallites in solution, where the aggregate sizes increased with increasing concentration confirming stepwise CPZ aggregation[31]. Barbosa *et al.* who used small-angle X-ray scattering and EPR spectroscopy also inferred that CPZ remained in solution as nanocrystallites[32]. We believe that for PTH and analogues to aggregate in solution stepwise implies heterocycle to heterocycle interactions, *i.e.* by excimerization, as confirmed by Mukerjee and Gosh, for the self-association of methylene blue into multimers[33] (figure 1B). PTH side chains serve to stabilize aggregation *via* solvent enforcement[31]. At nanostructural levels, CPZ in solution answers to the demands of solid state characteristics[34,20 and 32].

Impurity centres

RSC Advances Accepted Manuscript

In aggregates of PTH, intermolecular charge transfer complexing is a way of aiding electron delocalization, just as the addition of a foreign molecule as an impurity centre does[34,20 and 35]. We regard the PL as such an impurity centre. An aggregate structure of this kind results in a considerable contribution to the free energy of the system. At 300°K, this free energy gain is about 0.055 log*N* eV. In a monolayer of just 20 molecules, the energy gain is quite substantial, about 0.072 eV. *cf.,* the approximate hydrogen bond value of 0.08 eV in bulk water[20]. The clearest feature of an excimeric charge transfer complex is the reversibility of equilibrium with its isolated components, according to the reaction scheme (second and third step) in Equation (1) (from [20]):

$$\begin{aligned} &D\ (\text{donor}) + A\ (\text{acceptor}) \Leftrightarrow DA\ (\text{contact CT}) \Leftrightarrow \\ &DA^{*}\ (\text{exiplex or excimer}) \Leftrightarrow D^{+}{-}A^{-} \Leftrightarrow D^{+} + A^{-} \end{aligned} \quad \textbf{(1)}$$

For an excimer $D^{*} = A^{*}$

Energy differences involved in such excitation processes are generally small, even of the order of kT, and can therefore be produced by a variety of supplying mechanisms, (including electrochemical phenomena at membrane surfaces)[36 and 37], with profound consequences for electron transfer processes in the presence of PTH[20]. For high stability, charge transfer should be incomplete[38]. Excimeric electron affinity is increased if the electron is taken not to the bottom of the conduction band but into an excited state energy level leading to enhanced complexation. If the electron is raised not from the Fermi level but from a higher excited state energy level, the ionization potential is reduced leading again to enhanced complexation. Both processes may occur simultaneously. Excimeric charge transfer complexes play important roles in many biological processes[20]. A corollary of aqueous assemblages of such particles is that counter-ions and water molecules are attracted by the hydrophilic regions, and assume extensively ordered states. Excitation also leads to considerable changes in magnitude and direction of dipole moments[39 and 40].

pH effects

Self-association of PTH reduces the pH of the cationic drug assembly such as seen for PMZ, CPZ and thioridazine (TDZ)[29], [41 and 42]. Furthermore, all PTH/PL adducts were more acidic in PTH concentrations equivalent to the pure drugs. The straight line plots in Figure 3, in which the hydrogen ion concentration differences ($[\Delta_i H^+]$) *vs* MR show a regular increase, is evidence that the PTH/PL adducts have specific, and similar, structures. (Definition: $[\Delta_i H^+] = [H^+]_{PTH/PL} - [H^+]_{PTHpure}$ at equimolar PTH concentrations). Within the cohorts of PL, with different headgroup but the same Ci, the plots for the smaller Ci show concomitant smaller $[\Delta_i H^+]$ increases as exemplified in Figure 3. This Figure shows that $[\Delta_i H^+]$ is strongly dependent on the acyl chains. The $[\Delta_i H^+]$ increase as a function of MR increase indicates that the protonated side-chains of the adduct PTH molecules orient away from the hydrophobic PTH/PL core, and thus structure the immediately adjacent (vicinal) water environment and by extension, lower the pH of the bulk solution. Water-assisted aggregation forces the PTH molecules into higher-order ion clusters, increases the dielectric environment, hence forcing the proximity of the heterocyclic ring donor and ring acceptor groups. This is expected to strengthen charge transfer excimerization[20]. The PL acyl chains are then also forced into closer proximity by the hydrophobic PTH ring assemblies. The plots indicated that the different PL headgroup interacted with the PTH in a closely similar manner irrespective of whether the PL were zwitterionic or salts. Note that the points on each line in Figure 3 again follow the PL MR hierarchy as seen in Figure 2 (PS > PE > PA).

Influence of the headgroup

Yeagle claims that PL headgroup and acyl chains may be treated as being partially independent of motion and may thus be treated separately[43]. In terms of imbibing water, *i.e.* water binding, eggPE < eggPS < eggPC, follows the hierarchy of CPZ/PL MR *vs* PL MW [44 and 45] (figure 2). A single methyl group added to PE (PE Me) sees a 28% increase in hydration while successive methylations increase the hydration by 7% and 16%, respectively[46 and 47]. Such hydration increases are also seen for successive methylations of dioctanoyl-PE and dimyristoyl-PE [48, 49 and 50]. We thus infer that full PL hydration is observed in all our experiments. Solubility of the PL as a function of the headgroup plays a major part in the MR hierarchy shown in figure 2. PC is the most soluble of the groups in figure 2 and phosphatidic acid (PA) the least, reflected in increasing MR according to the adducts with the same diacyl chains in the order PC < PG < PS < PE < PA. Not only is solubility a factor but the adducts of PL with larger headgroup volume have smaller $[\Delta_i H^+]$ (figure 3). All the PTH/PL interactions exhibit similar $[\Delta_i H^+]$ changes. This suggests that the initial site of adduct formation is situated nearer the α part of the diacyl chains than the headgroup (figure 1C). A larger dynamic headgroup as well would provide more steric hindrance to the initial PTH anchoring site. This is seen for the series in Figure 4 in which the headgroup size increases by virtue of methyl additions 16PE < 16PENMe < 16PEN2Me < 16PC whose MR fall on the 16PL line in Figure 3, and concomitantly exhibit smaller $[\Delta_i H^+]$ in that order.

Influence of the diacyl chains

Figures 2 and 3 show unambiguously that longer diacyl chains elicit larger PTH/PL MR. Taking into account the steric hindrance of the headgroup, the MR for PTH/PL is an index of the lipophilicity of the PL in question. Thus, for example, PA, the most lipophilic of the PL in our experiments, must acquire a larger quantity of PTH for its adducts to become water-soluble, as indeed is observed. This phenomenon may be explained by placing the lipophilic portion of the PTH nearer to the initial anchoring site of PA namely at α in its diacyl chains (figure 1C). Further, to render the adduct soluble, more PTH has to be marshalled to that site. In tum, as the length of the diacyl chains is increased, the PTH excimeric ribbon must be extended to cope with the increasing lipophilicity of the PL until a point is reached where the splay and motion of the diacyl chains overcomes the cohesive excimeric and the vicinal water structure energetic regimes that keep the adducts soluble. This usually occurs when an MR of about 40 to 50 is reached. This view explains why the adduct of CPZ/24PC (MR 53) CPZ/18PS (MR 38) and CPZ/16PE (MR 46) precipitate overnight, while CPZ/18PA (MR 78) precipitates within several hours (see the underlined MR in table 2A).

Sedative effects

Some workers claimed that the sedative effect of clinical doses of psychotropes for stereospecific site interaction increased in

RSC Advances Accepted Manuscript

the order PMTZ < PMZ < CPZ < PClP < TFP ("Series 1" first row in table 1)[51 and 52]. PTH charge transfer complex order depends on the electron withdrawing power of the substituent in the heterocyclic 2-position, $-CF_3$ > -Cl > -H, with consequent increasing ionization potential (I_p) [53 and 54] as well as flexibility of the molecules[52]. Fulton and Lyons suggested that the increasingly sedative effect of PTHs tended to follow their decreasing ionization potential I_p [47]. However, they emphasised caution in this respect, because there was little difference between tranquilizers or stimulants. A smaller I_p allows for an easier loss of an electron in a charge transfer event. But, it is necessary to bear in mind that charge transfer in excimer context is a probability process in which the electron may not actually be lost by the donor but may spend more time near the acceptor. Thus, physiological activity does not depend on electron donor power alone. Conformational factors and the lipophilicity-influencing activity of psychomimetic drugs has been discussed extensively[9,55,56,57 and 58].

Non-neuronal effects

Our MR data are at odds with the sedative clinical information above and may indicate non-neuronal aspects. The PTH aromatic rings are capable only of butterfly wing motion about the N-S axis, rarely if ever inverting, whereas the side-chains are flexible depending on length and substituents. When conformational factors of the PTH in its PL adducts are examined, their correlation with MR becomes evident. This is PC< PG < PS < PE < PA and referred to as "Series 2" (table 1, first column). While series 2 is concerned with PTH/PL adducts only, this nevertheless leads to a possible insight into other clinical effects. PMTZ has a methyl substituted in the two-carbon side-chain and thus will have a less flexible side-chain. PMZ, CPZ and TFM share a simple propylamine side-chain. While the strength of the electron withdrawing groups in the ring 2-position plays an important role, the sizes of those groups also increase in the order H < Cl < CF3, inducing a steric hindrance effect that may affect excimerization. The perazines have a piperazinyl side-chain that is longer than the simple propylamine group. Moreover, the piperazinyl group introduces two quatemizable N atoms, leading to boat or chair conformations depending on whether one or both are protonated[58]. The perazine boat form (mono-H^+) is preferred at a pH of approximately 5, *i.e.,* within the conventional clinical range of PTH with a propylamine side-chain. The di-protonated piperazinyl chair form exists in the pH range of about 3 [58]. Table 1 shows that TFP•HCI (boat form) has a considerably lower MR than the chair form TFP•2HCl for 16PC, indeed invariably so for all TFP/PC adducts with corresponding Ci tested. There is no doubt that this phenomenon involves vicinal water which is less structured for the chair than the boat form. We suggest the psychomimetic effect follows Series 1 until the available stereo-specific sites are occupied or even saturated, after which the unused excess PTH are exposed to PL in non-neuronal terms (i.e. in "Series 2" order table 1: PC > PG > PS > PE > PA). The process for self-associated PTH accumulation at membranes has thus several avenues available for interaction. The tertiary PTH interaction is mainly at intrinsic proteins; quatemized PTH interact only with phospholipids[59]. The relatively distinct sets of physiological action can now be ascribed to one series (Series 1) involved with neurolepticity requiring a specific conformation of a single PTH at a stereoselective protein site, and to another *(*Series 2) with a much more generalized interaction of a PTH pseudopolymer at available membrane PL sites. Overlap of Series 1 and 2 is yet to be determined.

Putative PTH/PL structure

The conventional view of amphipathic PTH aggregates being spheroidal, ellipsoidal, cylindrical or disc-shaped may not apply in our case[60]. A recent study of the self-assembly of PTH compounds was inconclusive with respect to the assignment of three-dimensional models: ellipsoids, cylinders or parallelepipeds[32]. Although at low concentrations the aggregate structure may approximate the Hartley spherical model, this is not likely to prevail in more concentrated solutions, as confirmed by streaming double refraction and x-ray diffraction measurements[32]. In the mixed PTH/PL systems, different three-dimensional criteria are likely to come into play, as has been observed with aggregates of PL and other ionic and non-ionic surfactants. See for example the work of Almgren who observed lace-like or thread-like structures for CPZ without intermediates in the form of disks[61]. Zuchowski and Durand showed that cationic PTH amphipaths interacted with artificial and biological membranes so that after the amphipath entered into the membrane a new type of interaction occurred[62]. Zhao's group, working with paclitaxel (an anticancer compound with an ionisable tertiary N group), showed incorporation of the drug into PL models differently with respect to headgroups, alky 1 chain lengths and unsaturation[63,64 and 65].

Recently, Kopec and Khandelia have carried out some computer-assisted predictions of interactions between the anti-tuberculosis candidate drug thioridazine and two different model bilayers (a zwitterionic POPC (1-palmitoyl-2-oleoyl-sn-glycero-3-phosphocholine) and a negatively charged, mixed POPC / POPS (1-palmitoyl-2-oleoyl-sn-glycero-3-phospho-L-serine)[66]. They have made a number of predictions that are coherent with the ideas presented here. Firstly, they have proposed that the positively charged protonated amino group of THZ's piperidine ring interacts with both the lipid headgroup and the glycerol backbone region via electrostatic interactions (salt bridges) and/or hydrogen bonds similar to that illustrated in figure 1C. Secondly, they predict that the preferential orientation of the molecule with the phenothiazine ring placed almost perpendicularly to the bilayer, again as seen in figure 1C. They also note that this is the preferred orientation of cholesterol[67]. Finally, they note that the strong interaction of the piperidine ring with the lipid phosphate group and glycerol backbone, will limit the conformational possibilities of the aromatic tricycle, making a parallel alignment highly unfavourable. This is in agreement with the hypothesis proposed here where the aromatic tricyclic rings are only partially overlapped. This, the fold and the tilt angle (figure 1B) will provide separation in three dimensions for the piperidine ring.

Phospholipid splay angles

If one considers for simplicity the PTH to be arranged in circular rings, then by calculating the difference between the MR for increasing Ci steps, then one can obtain a rough estimate of the number of CPZ molecules which bind to the additional chain length of the PL (table 3). Knowing this, one can calculate the fold angle around the S-N axis (figure 1B).

RSC Advances Accepted Manuscript

In geometric algebra terms, the sequence of numbers in table 3 can be considered as a source for providing progressive values of 2D orthogonal projections of molecular locations on the spiral pathway on to a flat surface, the values of which determine the splay angle and pitch of the spiral (cf. an inverse problem in mathematics or time consuming analysis).

Assuming the CPZ eximer to be fully overlapped then the length Q (figure 1B) can be used to calculate the effective length of the sides of the polygon descried by the PTH molecules. The absolute length for Q varies from about 2.75-3.25 Å depending on which source is used (CSR space filling or ChemDraw models of various PTH derivatives). Its absolute length will be reduced to an effective length because of the fold and the thickness of the carbon ring. An absolute length of 3Å is used for the calculations presented in table 3 (although other values in the 2.75-3.25 Å range do not result in significantly different conclusions). Once the length of the polygon edge formed by the CPZ is known it is possible to calculate the radius of the inscribed circle. Yeagle (Chapter 1, tables 1-7) gives cross-sectional areas of several different phospholipid chains, which can be used to provide an averaged area of 38.05 $Å^2$ [43]. Using the radius of the phospholipid chain thus to be 3.48Å, it is then possible to calculate the splay angle of the phospholipid chains. Once again it is possible to see that the series 2 order is maintained (PC < PE < PA) when the splay angle is compared to the chain length (figure 5).

Returning to the spiral concept presented in figure 1C, it would appear that at longer chain lengths, due to the splay angle of the phospholipid chains, that the spiral is in fact some sort of helix (Figure 6). This could be anticipated considering the tilt and fold angles of the PTH molecule. From the data available to us, it is not possible for us to decide whether the helix has one or more threads around the central phospholipid chains and so table 3 gives splay angles for a single or two threads as examples.

One well-known series of numbers, often associated with a spiral in nature is the Fibonacci series (1, 1, 2, 3, 5, 8, 13, 21, 34, 55…) as seen in the seeds on a sunflower, the spirals of shells, and the curve of waves. In theoretical studies in the mathematics of fractals for constructions using triangles (in 2D), the results show that the Fibonacci sequences can be found in the gaps formed[68]. Here it is interesting to note that if the molar ratios determined here for all five PTH (PC, PG, PS, PE and PA) are plotted against this series, then one obtains straight line graphs with a correlation coefficient of greater than 0.987 in all cases (figure 7). It's significance was unclear until it was recognised as related to energy optimisation in 3D such as in some nature examples (e.g. spinal growth in some plant locations along a stem), However, this is one of the first observations of the Fibonacci series fitting at the molecular level.

Correspondence of PTH/PL and PL

In terms of cellular biosynthetic routes (precursor → product): PA → PG, PA → PI, PA → PS → PE → PENMe → PEN2Me → PC → SM[69,70 and 71], it is remarkable that product PTH/PL MR is almost always smaller than that of the precursor PTH/PL MR (the exception being PS → PE) see Table 1 and Figure 2. The MR indicates that fewer PTH molecules are used to enclose (and modify the properties of) PA than PS.

It has long been appreciated that lipid species are not distributed equally among the various cellular membranes[72 and 73] and that the membrane itself is asymmetric and has substructures including rafts[74]. In the outer leaflet in bacteria, after closely bound PE and cardiolipin (CL), the third major PL is PG. Van Meer, Voelker and Feigensohn produced an elegant article on the location, prevalence and distribution of PL within a eukaryotic cell[74]. In terms of concentration, and traversing the cell from outer cell membrane to the 'core' (endoplasmic reticulum and mitochondria) of the cytosol, the PL distribution tends to follow the Series 2 order, *i.e.* PC > PG > PS > PE > PA [22 and 74]. Interestingly, PE, and PS are preferentially located on the cytosolic side of the plasma membrane while sphingomyelin (SM) which is predominantly located in the outer layer (luminal side) of the plasma membrane. This gradation results in inner membranes being loosely packed while outer membranes are stiffer and closer to adopting a 'solid' gel phase.

Thus the PL most protected from external assault (treatment) by the PTH in eukaryotic cells is PA, which is also the precursor of ultimately all the PL products mentioned above. The next are PE, and PS. Thus the most PTH 'sensitive' PL are the PL which are the most protected and the least sensitive are the most exposed. This may well have important consequences for PTH treatment.

Tumour cells produce extra PG and PC and this apparently contributes to both proliferative growth and programmed cell death mechanisms[75]. PC, sphingomyelin (SM) and PG have also been found in higher proportions in various cancer cells[76]. This may present convenient targets for interaction with PTH.

Children with frequently recurring pyelonephritis responded better to combined PMTZ/antibiotic treatment than to antibiotics alone; and furthermore, no new renal scarring was observed in the PMTZ-tested group[20]. Free floating *E. coli* are likely destroyed first, while adherent pathogens are more tenacious because less surface area is exposed, PTH/PG still being involved.

Discussion,

If the PTH does form spiral metastructures around phospholipids, what would be the effects and consequences.

Considering the PTH molecule itself, the hydrophobic ring structures are reasonably flat and thus would presumably tolerate a reasonable amount of relative rotational movement. This would allow the variable pitch in the spiral needed for different splay angles (SA and p in figure 7 respectively).

While one would anticipate that the fold angle (figure 1B) would be quite inflexible, the effective fold angle may actually be augmented by allowing the hydrophobic ring structures to rock on each other. This is probably necessary in order to achieve the range in number of PTH molecules in the rings/spirals around the phospholipid (as given in table 3 column 'd').

The resolution of the molar ratios into straight lines by plotting them against the Fibonacci series is especially intriguing. It is interesting regarding Fibonacci numbers and the coverage of special sections. The generating function f(x) of the Fibonacci numbers satisfies the identity:

$$(1-x-x^2)\, f(x) = x$$

RSC Advances Accepted Manuscript

which leads to the closed form $t^n-(1-t^n)/\sqrt{5}$

where $t = (1+\sqrt{5})/2$ **(2)**

This is the so-called 'golden-mean' (or 'golden ratio') of identical copies of a fundamental structural unit cell oriented in the same way. This again suggests a highly ordered alignment of the PTH molecules around a central point.

The splay of the phospholipid itself induced by the PTH molecule would lead to a local membrane thinning and changes in membrane fluidity and functionality. Membrane thinning and expansion has been observed in other biological situations including binding to antimicrobial peptides and to PTH[66]. Antimicrobial peptides have been shown to produce perturbation of the phospholipid membrane by the formation of specific lipid–peptide domains, lateral phase segregation of zwitterionic from anionic phospholipids and even non-lamellar lipid phases[77]. Furthermore, some peptides change their topology in a pH dependent manner and these peptides have been shown to be more potent in antibiotic assays under experimental conditions where they show approximately in-plane alignments[78]. In an interesting study using four of the phospholipids used here (PC, PG, PS and PE), Sevcsik *et al.,* demonstrated that their interaction with the human multifunctional peptide LL-37 show that net charge of the lipid is not the decisive factor determining the membrane-perturbing mechanism of LL-37. The perturbation was induced by a combination of several parameters, including packing density, the ability to form intermolecular H-bonds, and the molecular shape of the lipid[79].

The organisation of the PTH molecules around a phospholipid impurity centre would also result in a uniformly charged annulus (where the actual charge depends upon the individual PTH molecule in question and the local pH). Without counter ions, this would be expected to induce a destabilising force between the individual PTH molecules, but it may also be this force repulsion that together with hydrophobic attractive forces between the ring structures and the acyl chains, helps push the PTH molecules deeper into the lipid bilayer in each successive turn of the helix.

The PTH and phospholipid molecule 'complex' will present a fairly large structure (extending up to approximately 60Å from table 3) and such a structure would also be expected to have a significant effect on the local membrane curvature strain, surface charge, fluidity, and melting point. This could be the basis for the observations that trifluoperizine forms drug-rich domains in membranes which in turn lead to the inhibition of the outward transport of anticancer drugs by the glycoprotein P (Pgp) in cancer cells[5 and 80]. Whether the changes in membrane properties are a result of incomplete miscibility as suggested by Cieslik-Boczula *et al*. or whether it is due to the molecular organisation suggested here has yet to be determined.

Depression of the membrane's melting point by anaesthetic molecules has been known for a long time. Recently, Græsbøll *et al.*, have described an general model to explain the anaesthetic features of arbitrary molecules in which they propose that 'anaesthetics are ideally soluble in the liquid phase of the membrane only and are insoluble in the solid phase[81]. Such a PTH and phospholipid molecule complex as described here would clearly have significantly different entropies in the liquid and solid states due to the 'accessibility' of individual phospholipid molecules.

Experimental

Gravimetric micro-titration

We used the simplest preliminary method, gravimetric micro-titration, to examine the behaviour of the PTH/PL interactions in water to avoid possible buffer or ion-adjusting salts effects, particularly in view of the fact that PTH behave as buffers in microclimates. In addition we confined ourselves to PTH all in hydrochloride form to avoid anionic differences[52].

Reagents

Reagents were used as received. The PTH•hydrochlorides (figure. 1A) came from Sigma Chemical Co., and all were infinitely water-soluble for our experimental purpose. Avanti Polar Lipids supplied natural product extracts, as well as all the purified (99% or better), synthetic 1, 2-diacyl-sn-glycero-3 -phospholipids (PL) with different headgroups (HG), and with even-numbered, symmetric, saturated diacyl chains varying generally from 8 to 24 carbon atoms per chain. Such numbers are indicated variously as iC or Ci, *e.g.,* 16PL or C16. The PL headgroups were choline (PC), ethanolamine (PE), the mono-sodium salts of phosphate (PA), *rac*-1 -glycerol (PG), and L-serine (PS). Other PL were 16 -methyl-substituted PE (16PE Me, 16PE 2Me). Natural product extracts were: *Eschericia coli* B, egg- and brain- sphingomyelin, (ESM) and (BSM) respectively, and phosphatidyl inositol (PI). PL mol weights may be found in the Avanti Products Catalogue Revised VI (homepage, www.avantilipids.com), that also gives extract compositions used here.

Equipment

Denver A200DS balance (10^{-5} g), Oakton 1000 pH meter (0.01), (6 mm) Accumet pH electrode, Haake circulating pumps, Cole-Parmer 8848 ultrasonic bath, silanized microsyringes, 15 mL silanized glass vials with Bakelite screw-caps, the latter never in contact with mixtures and solutions. The silanization product was Dow Coming MDX4-4159 Fluid provided by Factor II, Inc. P.O. Box 1339, Lakeside, Arizona 85929.The vials were silanized to obviate the negative surface charge on glass, also found on membranes and vesicular surfaces, that could affect the course of PTH/PL aggregation[20 and 35].

Procedure

Water was added to accurately weighed PL powder (in the range of 1-3 mg) yielding ultimately ~10^{-5} M, (i.e. within an order of magnitude of the 10^{-6} M critical micel concentration (CMC) of biological PL, most of which have two long acyl chains [17]). Moreover, the PL were thus fully hydrated (see later). The suspension was subjected to sonication and heating to several degrees Celsius beyond the corresponding PL phase transition temperatures[82]; sonicated again at 37°C; cooled to 0 °C; again sonicated at 37°C; and then incubated at 37°C, (each step for 1-3 min). PTH solution (~0.15 M) was added by micro-syringe in weighed increments, the mixture subjected to the above temperature cycle, and addition and cycling repeated until turbidity cleared, which was taken to be the adduct

RSC Advances Accepted Manuscript

endpoint and expressed as the PTH/PL molar ratio (MR). The solution was clear in a temperature range of several degrees Celsius on either side of the MR. After each incubation, the vial and contents were allowed to reach room temperature, upon which the vial (externally) and cap (internally and externally) were dried with lintless tissue, and the assembly tared for further additions of PTH. At room temperature and MR, the pH of the adduct solutions was compared to that of the equivalent pure PTH concentration (for relatively soluble PL with small iC-numbers (see Avanti Catalog). After the MR had been reached and the pH taken, the PTH/PL mixtures were stored in the dark for evaluation of colour production, and possible reprecipitation.

Conclusions

We have presented data to illustrate that the interaction products of PTH and PL are water-soluble and stoichiometric, their molar ratio (MR) following a defined order of the headgroups (Table 1). Within this group must be counted phosphatidyl ethanolamine-mono-methyl (PENMe) and phosphatidyl ethanolamine-di-methyl (PE 2Me). The MR *in vivo* interaction products PTH/PL are always smaller than the PTH/precursor PL. The hydrogen ion concentration increase $[\Delta_i H^+]$ is always larger for the PTH/PL than for the equivalent pure PTH concentration $[\Delta_i H^+]$ and is strongly dependent on the diacyl chain length. Each chain length in Figure 3 contains all the PTH tested in the order given above. This confirms Yeagle's claim of partial independence of the headgroup and the acyl groups of a PL[43].

Finally the reproducibility of the molar ratio suggests that PTZ and PL interact in a defined matrix as adducts and not as loose aggregates. Since the results for all the various PTZ always retained the series 2 order, this suggests that the adducts formed are similar in all cases. Therefore we have used the molar ratios and knowledge about the forces between the molecules to propose that a phospholipid can act like an impurity centre around which PTZ can form a helix. If the chain length is sufficiently long and the headgroup small, the two lipid chains can splay to maximise the hydrophobic binding. The correlation between the molar ratio and the Fibonacci series suggests that the adducts formed are well organised to minimise energy relationships.

Comparison of the data obtained here with the known therapeutic effects of these derivatives leads to the observation that the therapeutic phenothiazine derivatives (PTH) can be divided into two overlapping groups. One of these (referred to here as Series 1) is psychotropic and based on heterocyclic ionization potentials. The other (Series 2) is based on lipophilicity and relates to the non-neuronal effects on cellular membrane phospholipids which results in their therapeutic effectiveness against deleterious micro-organisms and cancer cells.

Acknowledgements

We thank Elysia Thornton-Benko for her support and medical information on micelles and stability during the early period of the project, and we thank Vivian C. Flores for her assistance to complete the manuscript.

Notes and references

[a] Department of Chemistry and Biochemistry, California State University, Los Angeles, 5151 State University Drive, Los Angeles, California 90032.
[b] Department of Biochemistry and Molecular Biology, University of Southern Denmark, Campusvej 55, DK-5230 Odense M, Denmark. sjf@bmb.sdu.dk.
[c] University of Technology, Sydney, School of Mathematical Sciences, and the School of Physics, University of Sydney, NSW, Australia. fthornton@ozemail.com.au
[d] MEMPHYS, Department for Physics, Chemistry and Pharmacy, University of Southern Denmark, Campusvej 55, DK-5230 Odense M, Denmark. jette-e-k@mail.dk or malthe@dadlnet.dk

†The ideas in this manuscript were pioneered by H. Keyzer. We have completed and submitted the manuscript posthumously in his honour.

* these authors contributed equally to the work
# to whom correspondence should be addressed.

Abbreviations

CL	chain length
I_p	ionization potential
MR	molar ratio
PL	phospholipid
CPZ	chlorpromazine
PClP•HCl	prochlorperazine•HCl
PClP•2HCl	prochlorperazine•2HC1
PMTZ	promethazine
PMZ	promazine
PTH	phenothiazine hydrochloride derivatives
TFM	triflupromazine
TFP•HCl	trifluoperazine•HCl
TFP•2HCl	trifluoperazine•2HCl
PA	phosphatidate (or phosphatidic acid)
PC	phosphatidylcholine
PE	phosphatidylethanolamine
PENMe	PE16Nmethyl
PENMe2	PE16Ndimethyl
PG	phosphatidyl glycerol
PS	phosphatidylserine
CaL	Cardiolipin

References

1. J. E. Kristiansen, O. Hendricks, T. Delvin, T. S. Butterworth, L. Aagaard, J. B. Christensen, V. C. Flores and H. Keyzer, *The Journal of antimicrobial chemotherapy*, 2007, **59**, 1271-1279.
2. G. Spengler, J. Molnar, M. Viveiros and L. Amaral, *Anticancer research*, 2011, **31**, 4201-4205.
3. M. J. Ohlow and B. Moosmann, *Drug discovery today*, 2011, **16**, 119-131.
4. A. Jaszczyszyn, K. Gasiorowski, P. Swiatek, W. Malinka, K. Cieslik-Boczula, J. Petrus and B. Czarnik-Matusewicz, *Pharmacological reports : PR*, 2012, **64**, 16-23.
5. G. Spengler, D. Takacs, A. Horvath, Z. Riedl, G. Hajos, L. Amaral and J. Molnar, *Anticancer research*, 2014, **34**, 1737-1741.

RSC Advances Accepted Manuscript

6. D. Zong, K. Zielinska-Chomej, T. Juntti, B. Mork, R. Lewensohn, P. Haag and K. Viktorsson, *Cell death & disease*, 2014, **5**, e1111.
7. D. Takacs, P. Cerca, A. Martins, Z. Riedl, G. Hajos, J. Molnar, M. Viveiros, I. Couto and L. Amaral, *In vivo*, 2011, **25**, 719-724.
8. S. Sharma and A. Singh, *Expert opinion on investigational drugs*, 2011, **20**, 1665-1676.
9. P. K. Dea, H. Keyzer and J. S. Maurer, in *Phenothiazines and 1,4-Benzothiazines*, ed. R. R. Gupta, Elsevier, New York, 1988, pp. 587-625.
10. P. M. Seeman, *Pharmacol. Rev.*, 1972, **24**, 583-655.
11. J. Hyttel, J. Arnt and K. P. Bøgesø, *Antipsychotic drugs: Configurational stereoisomers*, CRC Press, Boca Raton, Florida. , 1984.
12. J. Schmutz and C. W. Picard, in *Psychotropic Agents. Part I: Antipsychotics and Antidepressants*, eds. F. Hoffmeister and G. Stille, Springer 1980, vol. 55 (1), pp. 3-26.
13. S. J. Fey and K. Wrzesinski, *Toxicological sciences : an official journal of the Society of Toxicology*, 2012, **127**, 403-411.
14. M. J. Allen, *Electrochim Acta*, 1966, **11**, 1503-1504.
15. M. J. Allen, *Electrochim Acta*, 1967, **12**, 563-568.
16. J.-C. Pechere, *Abstracts of the Seventh European Congress of Chemotherapy and Infection, Florence, Italy, 2005*, 2005, **Abstract EL 1,** , 19-22.
17. M. W. Goosey and N. S. Doggett, *Biochemical pharmacology*, 1983, **32**, 2411-2416.
18. F. Gutmann, C. Johnson, H. Keyzer and J. Molnar, *Charge Transfer Complexes in Biological Systems* Marcel Dekker, New York, 1997.
19. K. Michalak, O. Wesolowska, N. Motohashi, J. Molnar and A. B. Hendrich, *Current drug targets*, 2006, **7**, 1095-1105.
20. M. R. Fernandez, H. Keyzer, M. Dea and P. K. Dea, in *Thiazines and Structurally Related Compounds. Proceedings of the Sixth International Conference on Phenothiazines and Structurally Related Psychotropic Compounds, Pasadena, Sept 11-14, 1990*, eds. H. Keyzer, G. M. Eckert, F. I.S. and G. R.R., Krieger Publishing Company, 1992, pp. 187-191.
21. A. I. McMullen and J. A. Stirrup, *Biochimica et biophysica acta*, 1971, **241**, 807-814.
22. P. Maher and S. J. Singer, *Biochemistry*, 1984, **23**, 232-240.
23. C. D. Francesco and M. H. Bickel, *Chemico-biological interactions*, 1977, **16**, 335-346.
24. M. Ahmed, J. Hadgraft and I. W. Kellaway, *Int. J. Pharmacology*, 1983, **13**, 227-237.
25. R. M. Julien, *A primer of drug action* W.H. Freeman, San Francisco, 1975.
26. H. Keyzer, H. K. Kim and C. Varkey-Johnson, in *Thiazines and Structurally Related Compounds*, eds. H. Keyzer, G. M. Eckert, I. S. Forrest and R. R. Gupta, Krieger Publishing company, Florida, 1992, pp. 213-218.
27. M. C. Carey, P. C. Hirom and D. M. Small, *The Biochemical journal*, 1976, **153**, 519-531.
28. V. C. Flores, H. Keyzer, H. K. Kim and J. Molnar, *Anticancer research*, 2002, **22**, 959-967.
29. R. Welti, L. J. Mullikin, T. Yoshimura and G. M. Helmkamp, Jr., *Biochemistry*, 1984, **23**, 6086-6091.
30. R. L. Smith and E. Oldfield, *Science*, 1984, **225**, 280-288.
31. S. Tehrani, N. Brandstater, Y. D. Saito and P. Dea, *Biophysical chemistry*, 2001, **94**, 87-96.
32. L. R. Barbosa, R. Itri, W. Caetano, S. Neto Dde and M. Tabak, *The journal of physical chemistry. B*, 2008, **112**, 4261-4269.
33. P. Mukerjee and A. K. Ghosh, *J. Amer. Chem. Soc.* , 1970, **92**, 6403-6407.
34. R. J. Abraham, L. J. Kricka and A. Ledwith, *J. Chem. Soc. Chem. Commun.*, 1973, **8**, 282-283.
35. V. Flores, C. Varkey-Johnson and H. Keyzer, in *Thiazines and Structurally Related Compounds of Biological Significance*, ed. J. Barbe, Enlight Assoc. , San Gabriel, USA, 1994.
36. B. S. Thornton, *Physics Letters*, 1984, **106A**, 198-202.
37. J. Molnar, B. S. Thornton, E. Thornton-Benko, L. Amaral, S. Zsujsanna and M. Novak, *Current Cancer Therapy Reviews*, 2009, **5**, 158-169.
38. H. Hauser and G. Poupart, in *The Structure of Biological membranes*, ed. P. Yeagle, CRC Press, Boca Raton, 1992, pp. 3-72.
39. D. Voet and J. G. Voet, *Biochemistry*, 2 edn., Wiley and Son New York, 1995.
40. L. Vroman, in *Interfacial Phenomena in Biological Systems*, ed. M. Bender, Marcel Decker, New York, 1991.
41. J. R. Silvius, *Lipid-Protein Interactions*, Wiley and Son, New York, 1982.
42. M. J. Mercier and P. A. Dupont, *The Journal of pharmacy and pharmacology*, 1972, **24**, 706-712.
43. P. Yeagle, in *The Structure of Biological Membranes*, ed. P. Yeagle, CRC press, Boca Raton, 1997, pp. 157-174.
44. R. Knoesel, B. Gebus, J. P. Roth and J. Parrod, *Bull. Soc. Chim. France*, 1969, **1**, 294-301.
45. B. Gebus, R. Knoesel and J. Parrod, *Bull. Soc. Chim. France*, 1969, **1**, 290-294.
46. J. E. Bloor, B. R. Gilson, R. J. Haas and C. L. Zirkle, *Journal of medicinal chemistry*, 1970, **13**, 922-925.
47. A. Fulton and L. E. Lyons, *Aust. J. Chemistry*, 1968, **21**, 873-882.
48. S. H. Snyder and E. Richelson, *Proceedings of the National Academy of Sciences of the United States of America*, 1968, **60**, 206-213.
49. Q. Duncan, H. Keyzer and K. L. Young, in *Biological and Chemical aspects of Thiazines and Analogues*, eds. J. Barbe, H. Keyzer and J. C. Soyfer, Enlight Association, San Gabriel, California, 1995, pp. 131-140.
50. G. L. Jendrasiak and J. C. Mendible, *Biochimica et biophysica acta*, 1976, **424**, 149-158.
51. R. P. Rand and V. A. Parsegian, in *The Structure of Biological Membranes*, ed. P. Yeagle, CRC press, Boca Raton, 1977.
52. P. K. Dea and H. Keyzer, *Conformational and Electronic Aspects of Chlorpromazine in Solution*, Plenum Press, 1986.
53. S. M. Gruner, M. W. Tate, G. L. Kirk, P. T. So, D. C. Turner, D. T. Keane, C. P. Tilcock and P. R. Cullis, *Biochemistry*, 1988, **27**, 2853-2866.
54. S. Mulukutla and G. G. Shipley, *Biochemistry*, 1984, **23**, 2514-2519.
55. A. T. Florence, *Advances in Colloid and Interface Science*, 1968, **2**, 115-149.
56. A. T. Florence, *The Journal of pharmacy and pharmacology*, 1970, **22**, 1-9.
57. D. J. Vaughan and K. M. Keough, *FEBS letters*, 1974, **47**, 158-161.
58. A. T. Florence, in *Micellisation, Solubilisation and Microemulsions*, ed. K. L. Mittal, Plenum Press, New York, 1977, vol. 1, pp. 50-74.
59. B. Bondy, 1988.
60. V. Flores, H. Keyzer and J. E. Kristiansen, in *6th European Congress on Chemotherapy and Infection (Dec. 1-3)*, Paris, France, 2004, p. Abstract 669.
61. M. Almgren, *Biochimica et biophysica acta*, 2000, **1508**, 146-163.
62. A. Zachowski and P. Durand, *Biochimica et biophysica acta*, 1988, **937**, 411-416.
63. L. Zhao and S. S. Feng, *Journal of colloid and interface science*, 2004, **274**, 55-68.
64. L. Zhao, S. S. Feng and M. L. Go, *Journal of pharmaceutical sciences*, 2004, **93**, 86-98.
65. L. Zhao and S. S. Feng, *Journal of colloid and interface science*, 2005, **285**, 326-335.
66. W. Kopec and H. Khandelia, *Journal of computer-aided molecular design*, 2014, **28**, 123-134.
67. T. Rog, M. Pasenkiewicz-Gierula, I. Vattulainen and M. Karttunen, *Biochimica et biophysica acta*, 2009, **1788**, 97-121.
68. G. W. Grossman, *Applications of Fibonacci numbers*, 1997, **9**, 211-224.
69. G. M. Carman and G. S. Han, *Journal of lipid research*, 2009, **50 Suppl**, S69-73.
70. A. Nohturfft and S. C. Zhang, *Annual review of cell and developmental biology*, 2009, **25**, 539-566.
71. A. M. Cardozo Gizzi and B. L. Caputto, *IUBMB life*, 2013, **65**, 584-592.

RSC Advances Accepted Manuscript

72. A. Shevchenko and K. Simons, *Nature reviews. Molecular cell biology*, 2010, **11**, 593-598.
73. C. Bissig and J. Gruenberg, *Cold Spring Harbor perspectives in biology*, 2013, **5**, a016816.
74. G. van Meer, D. R. Voelker and G. W. Feigenson, *Nature reviews. Molecular cell biology*, 2008, **9**, 112-124.
75. N. D. Ridgway, *Critical reviews in biochemistry and molecular biology*, 2013, **48**, 20-38.
76. S. Piotto, A. Trapani, E. Bianchino, M. Ibarguren, D. J. Lopez, X. Busquets and S. Concilio, *Biochimica et biophysica acta*, 2014, **1838**, 1509-1517.
77. V. Teixeira, M. J. Feio and M. Bastos, *Progress in lipid research*, 2012, **51**, 149-177.
78. B. Bechinger, *Molecular membrane biology*, 2000, **17**, 135-142.
79. E. Sevcsik, G. Pabst, W. Richter, S. Danner, H. Amenitsch and K. Lohner, *Biophysical journal*, 2008, **94**, 4688-4699.
80. K. Cieslik-Boczula, P. Swiatek, A. Jaszczyszyn, P. Zawilska, K. Gasiorowski, W. Malinka and G. Kohler, *The journal of physical chemistry. B*, 2014, **118**, 3605-3615.
81. K. Graesboll, H. Sasse-Middelhoff and T. Heimburg, *Biophysical journal*, 2014, **106**, 2143-2156.
82. A. Harder and H. Debuch, *Chemistry and physics of lipids*, 1986, **39**, 65-71.

RSC Advances Accepted Manuscript

Table 1

MR PTH/Lipids*	PMTZ·HCl	PMTZ·HCl	CPZ·HCl	TFM·HCl	PCIP·2HCl	TFP·2HCl	TFP·HCl
16:0 PC	38.8	22.4	3.8	20.9	11.6	27.7	22.5
16:0 PG	49	29.1	9.5	25.8	30.6	56.5	
16:0 PS	66	33.3	22.2	32.1		**85**	
16:0 PE	76	**61**	29.1	**77**		**112**	
16:0 PA	**169**		**46.6**	**317**		**143**	
PI**	49	37	13	16		18	
BSM**			3.8				
ESM**			3.2				
E. coli B total**	127	86	22	87		145	
E. coli B Polar**	88	83	18	35		129	

Table 1. Molar Ratio (MR) for Phenothiazine:lipid extracts

* "Series 1" reads horisontally and "Series 2" reads vertically
** Extract compositions from Avanti Polar Lipids, Inc. Catalogue VI. Revised
PI: Phosphatidylinositol (MW 587): weight %; 33, 16:0 saturated; 46.8, 18:2 unsaturated
ESM: egg sphingomyelin: Area % FAME-GC/Fl; 16:0, 83.9; 18:0, 6.3; 20:0, 3.8; 24:0, 4.2
BSM: brain sphignomyelin: "%": 16:0, 1.7; 18:0, 45.5; 20:0, 5.1; 22:0 7.2; 24:0, 23.3
other unsaturated/undetermined
Underlining indicates that precipitation ensues after 2 - 24hrs at MR

E. coli B, Total extract: weight %; PE 57.5; PG 16.6; CaL (cardiolipin) 9.8, other 17.6
E. coli B, Polar extract: weight %; PE 67, PG23.2, CaL 9.8, other 0.
Adduct colour of extracts are blue for PMTZ and pink for all the others
Apparent mol weight of E. coli arbritrarily taken as 750/mol, being the rough average of equimolar PE14 and PG18. Other mol. Weights given as by Avanti.

RSC Advances Accepted Manuscript

Table 2

A	Molar ratio (MR)				
CL/MR	**PC**	**PG**	**PS**	**PE**	**PA**
4	0.27				
6	0.8	2.1	2.5	4.2	4.6
8	1.3	2.3	4	4.9	6.4
10	1.5	4.3	5	9.3	10
12	1.9	4.3	7.2	10.4	17.8
14	2.6	7.2	10.5	17.8	30.1
16	3.8	9.5	22.2	29.1	45.6
18	6.7	16.1	38.1	46.5	78
20	12				
22	26.7				
24	53				
16PE-Nme				14.8	
16PE-Nme2				5.5	

B		Molar ratio differences with increasing acyl chain length (ΔMR)				
CL/MR	**CL (average)**	**PC**	**PG**	**PS**	**PE**	**PA**
6-4	5	0.53				
8-6	7	0.5	0.2	1.5	0.7	1.8
10-8	9	0.2	2	1	4.4	3.6
12-10	11	0.4	0	2.2	1.1	**7.8**
14-12	13	0.7	2.9	3.3	**7.4**	12.3
16-14	15	1.2	2.3	**11.7**	11.3	15.5
18-16	17	2.9	**6.6**	15.9	17.4	32.4
20-18	19	**5.3**				
22-20	21	14.7				
24-22	23	26.3				
Partial sum ΔMR for (8 - 18)		5.9	14	35.6	42.3	73.4

Table 2. A) MR of PTZ/PL combinations and B) their differences with increasing acyl chain lengths

Table 2A

Underlining indicates that precipitation ensues after 2 - 24hrs at MR

Table 2B

Note that equal differences tend to fall on a diagonal (see for example the values in bold type)

RSC Advances Accepted Manuscript

Table 3

	a	b	CL Å	d	e degrees	e radians	f	g	g1 degrees	g2 radians	g3	R Å	i Å	j Å	j radians	k radians	k degrees	SA degrees	SA2 degrees
PC	19	20-18	22.77	4.3	48.14	0.84	0.74	2.23	41.86	0.73	0.90	2.49	-0.98	-0.04	-0.00	-0.04	-2.48	-4.95	-15.84
	21	22-20	25.3	13.7	76.86	1.34	0.97	2.92	13.14	0.23	0.23	12.52	9.04	0.36	0.01	0.37	20.93	41.86	6.42
	23	24-22	27.83	25.3	82.89	1.45	0.99	2.98	7.11	0.12	0.12	23.85	20.37	0.73	0.01	0.82	47.06	94.11	31.22
PG	15	16-14	17.71	1.3	-48.46	-0.85	-0.75	-2.25	138.46	2.42	-0.89	2.53	-0.94	-0.05	-0.00	-0.05	-3.05	-6.11	-16.9
	17	18-16	20.24	5.6	57.86	1.01	0.85	2.54	32.14	0.56	0.63	4.04	0.56	0.03	0.00	0.03	1.60	3.20	-19.0
PS	15	16-14	17.71	10.7	73.18	1.28	0.96	2.87	16.82	0.29	0.30	9.50	6.02	0.34	0.01	0.35	19.87	39.74	-2.0
	17	18-16	20.24	14.9	77.92	1.36	0.98	2.93	12.08	0.21	0.21	13.71	10.23	0.51	0.01	0.53	30.36	60.71	11.8
PE	13	14-12	15.18	6.4	61.88	1.08	0.88	2.65	28.13	0.49	0.53	4.95	1.47	0.10	0.00	0.10	5.56	11.13	-22.5
	15	16-14	17.71	10.3	72.52	1.27	0.95	2.86	17.48	0.31	0.31	9.09	5.61	0.32	0.01	0.32	18.47	36.94	-3.60
	17	18-16	20.24	16.4	79.02	1.38	0.98	2.95	10.98	0.19	0.19	15.19	11.71	0.58	0.01	0.62	35.34	70.68	16.4
PA	11	12-10	12.65	6.8	63.53	1.11	0.90	2.69	26.47	0.46	0.50	5.39	1.92	0.15	0.00	0.15	8.71	17.42	-24.9
	13	14-12	15.18	11.3	74.07	1.29	0.96	2.88	15.93	0.28	0.29	10.11	6.63	0.44	0.01	0.45	25.90	51.79	0.3
	15	16-14	17.71	14.5	77.59	1.35	0.98	2.93	12.41	0.22	0.22	13.31	9.83	0.56	0.01	0.59	33.72	67.45	12.0
	17	18-16	20.24	31.4	84.27	1.47	0.99	2.98	5.73	0.10	0.10	29.74	26.26	1.30	0.02	1.30	74.33	148.66	62.6

Table 3. Calculation of phospholipid diacyl chain splay angles from molar ratio differences between phospholipids of different chain length but the same head group.

Notes for columns

a carbon position in lipid chain is CL

b (CL-(CL-2)) flanking a in tables 2 and 3

CL Chain length from carbon postion a to carbon w . Thus, position 17 gives 8 segments times 2.53 Å/segment = 20.24

d ΔMR for b equals one more than the number of sides of polygon of CPZ. One is subtracted to accound of the overlap of the molecules.

e half of fold angle of CPZ, = ([90-(180/ΔMR))

f sin[e]

g length of CPZ polygon edge/2 = (average) equals (3 multiplied by f) = 3 x sin[e] in Å units.

g1, g2, g3 are conversions from degrees to radians, etc

R radius of circle inscribed in polygon d, equals g/tan(180/ΔMR): (g1,2 conversion of degrees to radians, etc.) (see fig. 8)

i equals R - r where r is the average cross-sectional radius of a phospholipid (PL) chain pair : r = square root (38/pi) = 3.4779 Å (see figs IC, 6 and 8)

j (i)/CL = sin(1/2 x splay angle converted to radians

k arcsin (j) (in radians and degrees)

SA 2 x k is Splay angle of lipid chain pair for a PL

SA2 The SA if there are two CPZ chains around a single PL

RSC Advances Accepted Manuscript

Figure 1

A) The therapeutic psychometric phenothiazine hydrochloride derivatives (PTH) used in this study.

B) PTH Geometry.

General headgroup structure illustrating the tilt angle induced by the difference in size of the S and N atoms.

Diagram of the 'fold angle' between the two benzene rings induced by the S and N atoms and the separation distance between two PTH molecules.

C) Diagram of the proposed helical interaction between the phospholipid (in grey) and the PTH (black). HG = head group, α - ω the first and last carbon molecules in the acyl tails.

Figure 2

Plot of the total molecular weight of the phospholipid against the molar ratio PTH/PL for the phospholipids with differing chain lengths (as given in table 2 with the following headgroups: ■ phosphatidylphosphate (PA); ▲ phosphatidylethanolamine (PE); ● phosphatidylserine (PS); ◆ phosphatidyl glycerol (PG, chain lengths); and ▼ phosphatidylcholine (PC). The range of acyl chain lengths used was in all cases 6-18 except for PC where it was 4-24. (n = 3).

Figure 3

Plot of the differences in the hydrogen ion concentration ($[\Delta iH^+]$) from pure PTH to PTH for some PTH concentrations versus PTH/PL molar ratio, per acyl chain for ■ C18 phosphatidylphosphate (PA, $R^2 = 0.97$); ▲ C16 phosphatidylethanolamine (PE, $R^2 = 0.99$); ● C14 phosphatidylserine (PS, $R^2 = 0.92$). (n = 3).

RSC Advances Accepted Manuscript

Figure 4

Plot of the differences in the hydrogen ion concentration ([ΔiH^+]) versus the number of methyl groups for C16 phosphatidylcholine. $R^2 = 0.98$ (n = 3).

Figure 5

Plot of the splay angle versus the chain length for ■ phosphatidylphosphate (PA, $R^2 = 0.96$); ▲ phosphatidylethanolamine (PE, $R^2 = 0.99$); and ▼ phosphatidylcholine (PC, $R^2 = 0.99$) (n = 3) calculated as shown in table 3.

Figure 6

The key definitions for a helix. α = splay angle; p = pitch; R = radius and θ circumferential angle.

Figure 7

Plot of the molar ratio PTH/PL for the phospholipids with differing chain lengths against the Fibonacci numbers from 3 to 55. Headgroups: ■ phosphatidylphosphate (PA, , $R^2 = 0.99$); ▲ phosphatidylethanolamine (PE, $R^2 = 0.99$); ● phosphatidylserine (PS, $R^2 = 0.98$); ◆ phosphatidyl glycerol (PG, $R^2 = 0.98$); and ▼ phosphatidylcholine (PC, $R^2 = 0.98$). The range of acyl chain lengths used was in all cases 6-18.

RSC Advances Accepted Manuscript

Figure 8

Diagram of key measurements for the splayed phospholipid.

A) Line T indicates the mid axis between the two acyl chains of the phospholipid of chain length CL (from α to ω). r = the circumferential diameter around one acyl chain. R = the radius of the bounding circle of the polygon.

B) Diagram of the relationship between r, R, the polygon and its bounding circle. The polygon and bounding circle are separated for clarity.

C) The splayed phospholipid. SA is the splay angle and δ is the difference 2R – 2r.

RSC Advances Accepted Manuscript

A

Some PTH molecules		R_1	R_2
Promazine	PMZ	H	$-(CH_2)_3-N(CH_3)\cdot 2HCl$
Clorpromazine	CPZ	Cl	$-(CH_2)_3-N(CH_3)\cdot 2HCl$
Triflupromazine	TFM	CF_3	$-(CH_2)_3-N(CH_3)\cdot 2HCl$
Promethazine	PMTZ	H	$-(CH_2)_2-(CH_3)-N(CH_3)\cdot 2HCl$
Trifluoperazine	TFP	CF_3	$-(CH_2)_3-N\frown N(CH_3)\cdot 2HCl$
Prochlorperazine	PClP	Cl	$-(CH_2)_3-N\frown N(CH_3)\cdot 2HCl$

B

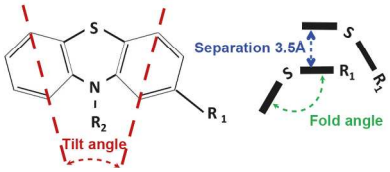

C

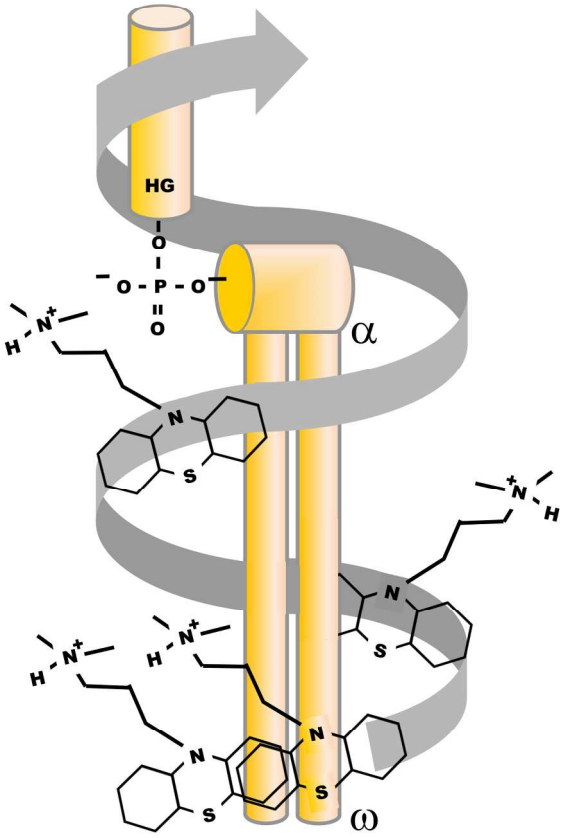

163x229mm (300 x 300 DPI)

RSC Advances Accepted Manuscript

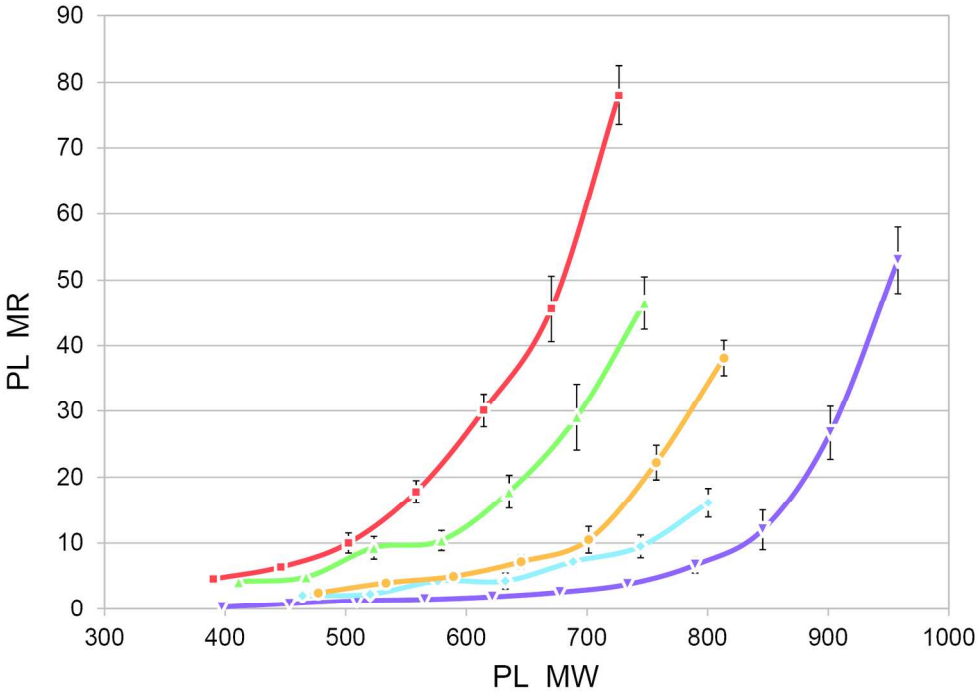

167x118mm (300 x 300 DPI)

RSC Advances Accepted Manuscript

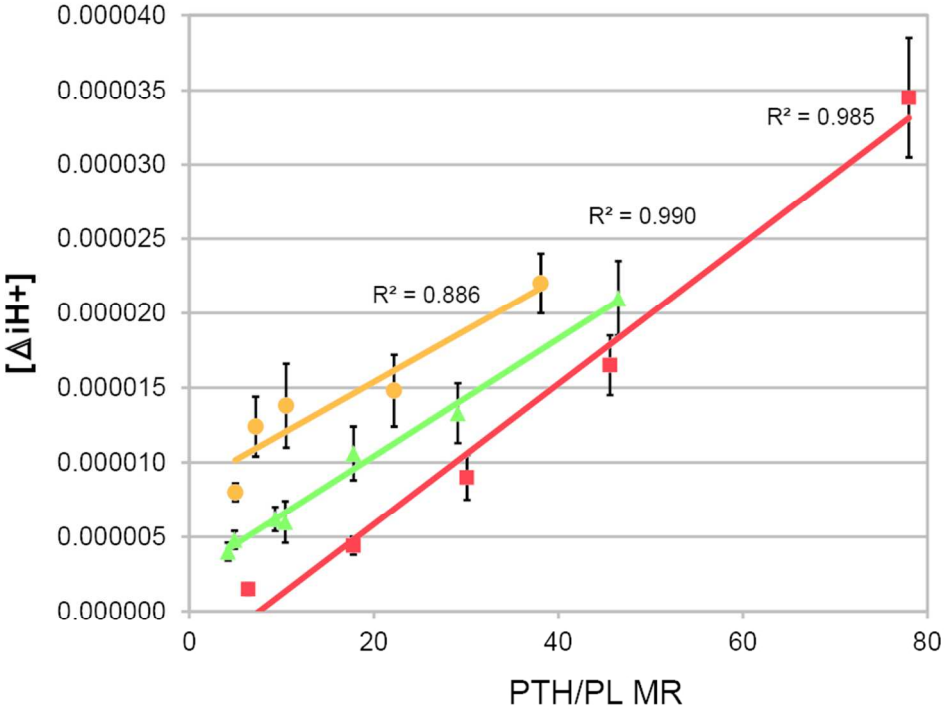

85x61mm (300 x 300 DPI)

RSC Advances Accepted Manuscript

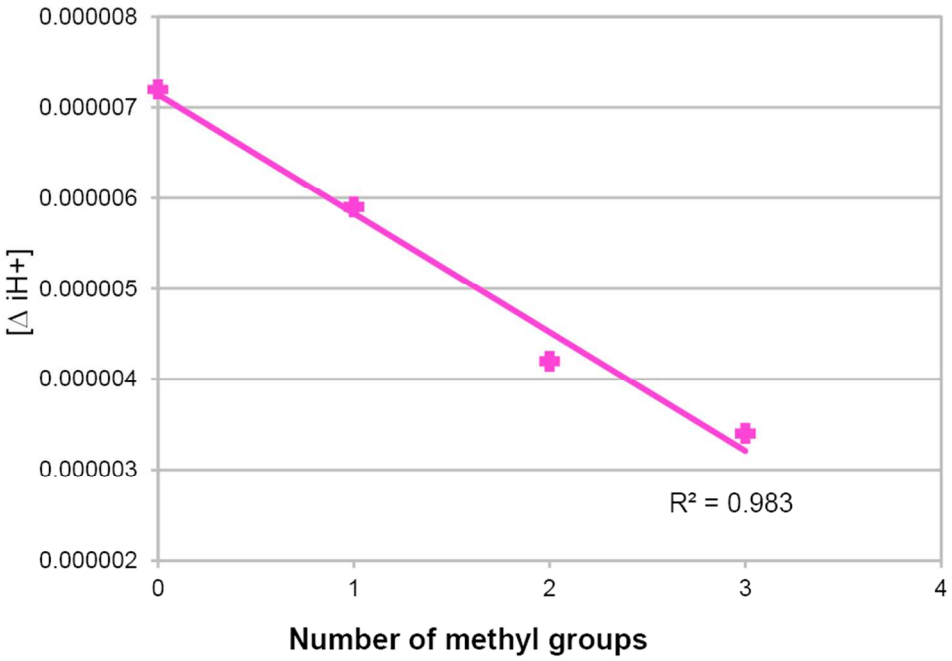

85x57mm (300 x 300 DPI)

RSC Advances Accepted Manuscript

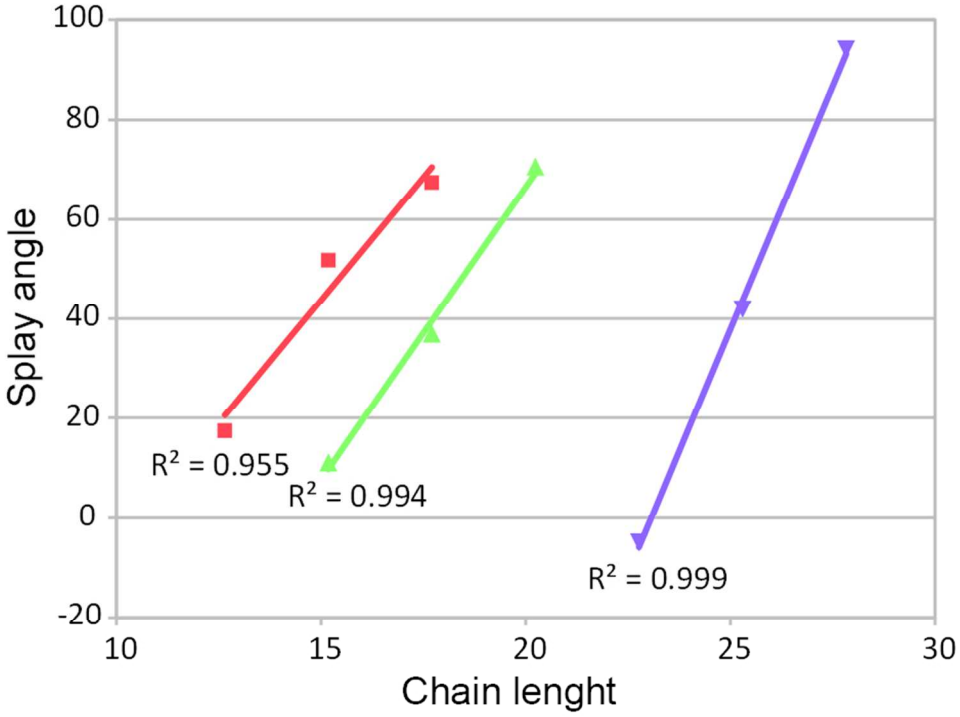

82x60mm (300 x 300 DPI)

RSC Advances Accepted Manuscript

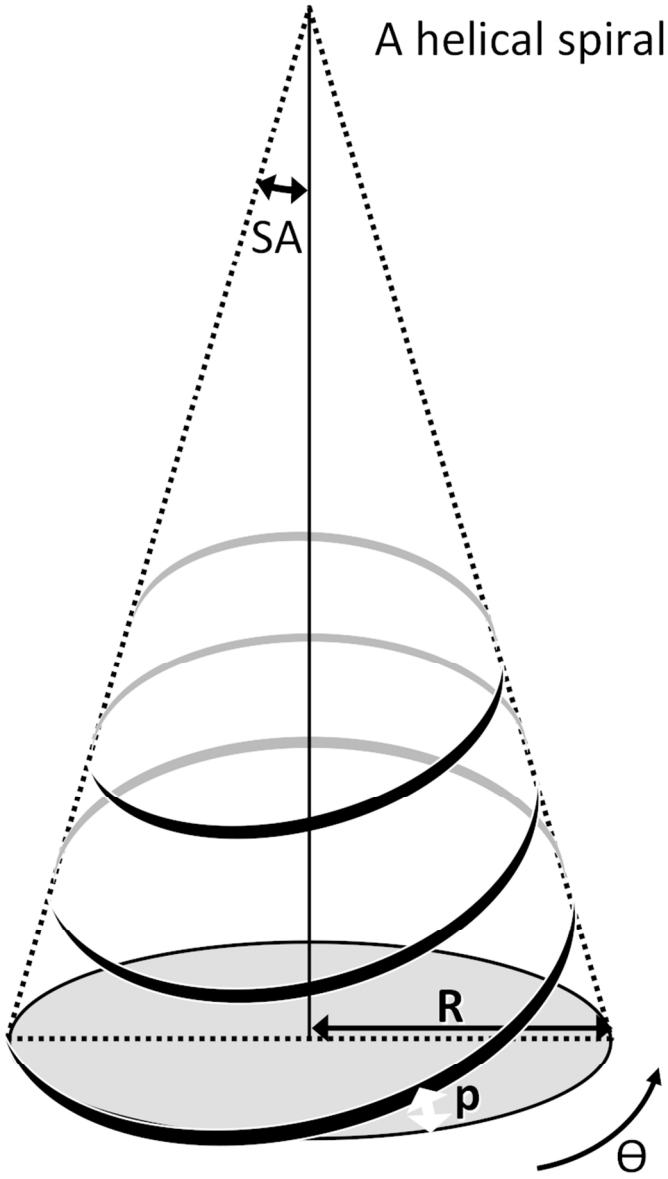

74x118mm (300 x 300 DPI)

RSC Advances Accepted Manuscript

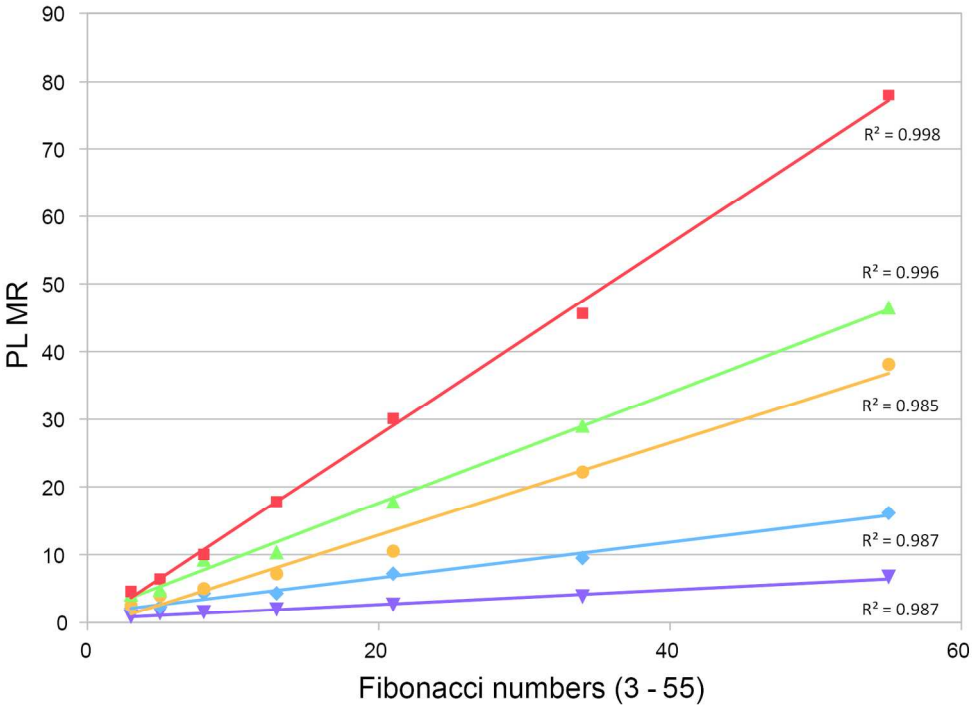

168x120mm (300 x 300 DPI)

RSC Advances Accepted Manuscript

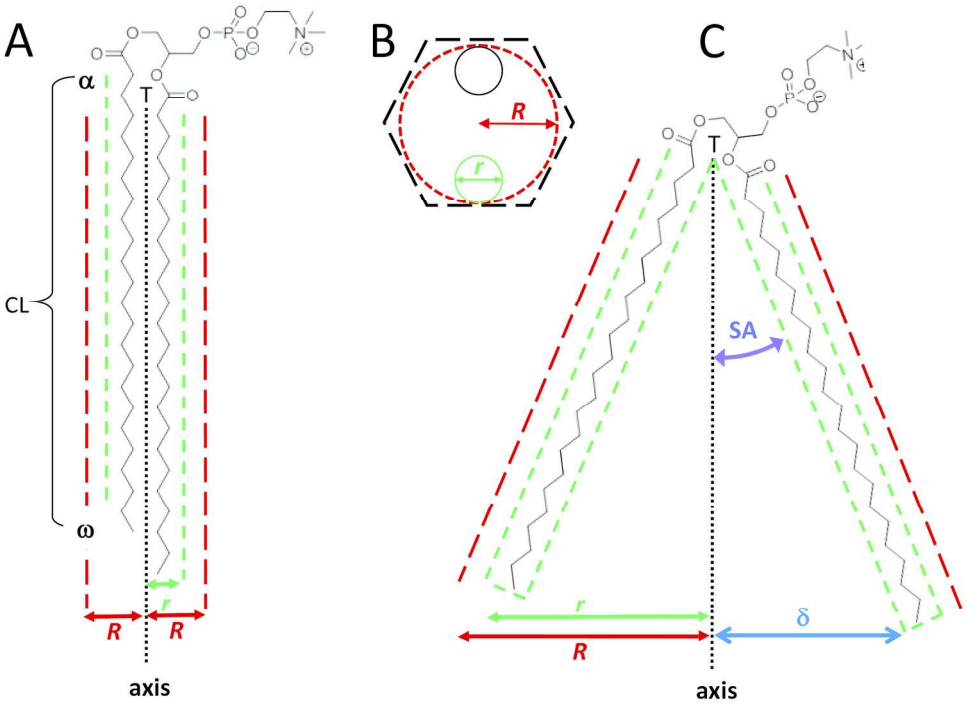

170x122mm (300 x 300 DPI)

RSC Advances Accepted Manuscript

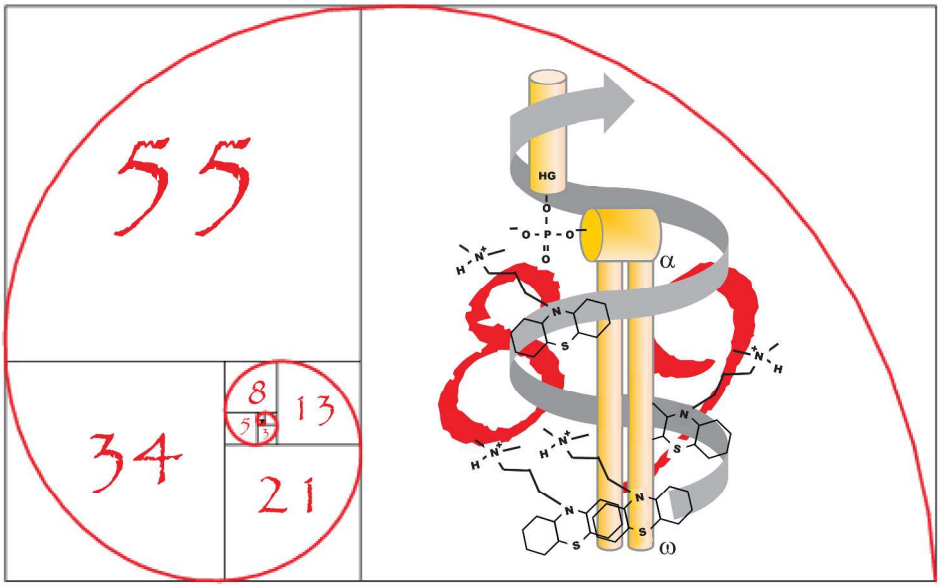

325x199mm (300 x 300 DPI)

RSC Advances Accepted Manuscript